THE JOURNAL OF BIOLOGICAL CHEMISTRY VOL. 290, NO. 14, pp. 9299–9309, April 3, 2015

COPS5 Protein Overexpression Increases Amyloid Plaque Burden, Decreases Spinophilin-immunoreactive Puncta, and Exacerbates Learning and Memory Deficits in the Mouse Brain*

Received for publication, February 10, 2015 Published, JBC Papers in Press, February 20, 2015, DOI 10.1074/jbc.M114.595926

Ruizhi Wang[‡], **Hongjie Wang**[‡], **Ivan Carrera**[§], **Shaohua Xu**[¶], **and Madepalli K. Lakshmana**[‡1]

From the [‡]*Section of Neurobiology, Torrey Pines Institute for Molecular Studies, Port Saint Lucie, Florida 34987, the* [§]*Department of Neuroscience, Euroespes Biotechnology, Poligono de Bergondo, Nave F, 15165A, A Coruna, Spain, and the* [¶]*Florida Institute of Technology, Melbourne, Florida 32901*

Background: Alzheimer disease (AD) is characterized by increased generation of amyloid β (Aβ) peptide in the brain.
Results: COPS5 overexpression increases Aβ, amyloid plaque burden, and learning deficits in a mouse model of AD.
Conclusion: As a RanBP9-interacting protein, COPS5 also plays a pivotal role in Aβ generation *in vivo*.
Significance: Targeting the COPS5-RanBP9 pathway may be an effective therapeutic approach for AD.

Brain accumulation of neurotoxic amyloid β (Aβ) peptide because of increased processing of amyloid precursor protein (APP), resulting in loss of synapses and neurodegeneration, is central to the pathogenesis of Alzheimer disease (AD). Therefore, the identification of molecules that regulate Aβ generation and those that cause synaptic damage is crucial for future therapeutic approaches for AD. We demonstrated previously that COPS5 regulates Aβ generation in neuronal cell lines in a RanBP9-dependent manner. Consistent with the data from cell lines, even by 6 months, COPS5 overexpression in APΔE9 mice (APΔE9/COPS5-Tg) significantly increased Aβ40 levels by 32% ($p < 0.01$) in the cortex and by 28% ($p < 0.01$) in the hippocampus, whereas the increases for Aβ42 were 37% ($p < 0.05$) and 34% ($p < 0.05$), respectively. By 12 months, the increase was even more robust. Aβ40 levels increased by 63% ($p < 0.001$) in the cortex and by 65% ($p < 0.001$) in the hippocampus. Similarly, Aβ42 levels were increased by 69% ($p < 0.001$) in the cortex and by 71% ($p < 0.011$) in the hippocampus. Increased Aβ levels were translated into an increased amyloid plaque burden both in the cortex (54%, $p < 0.01$) and hippocampus (64%, $p < 0.01$). Interestingly, COPS5 overexpression increased RanBP9 levels in the brain, which, in turn, led to increased amyloidogenic processing of APP, as reflected by increased levels of sAPPβ and decreased levels of sAPPα. Furthermore, COPS5 overexpression reduced spinophilin in both the cortex (19%, $p < 0.05$) and the hippocampus (20%, $p < 0.05$), leading to significant deficits in learning and memory skills. Therefore, like RanBP9, COPS5 also plays a pivotal role in amyloid pathology *in vivo*.

Alzheimer disease (AD)[2] is a devastating neurodegenerative disease of the elderly, affecting more than 35 million people worldwide (1). Neuropathologically, AD brains show extracellular amyloid plaques, intracellular neurofibrillary tangles, and marked atrophy in the brain (2). Amyloid plaques results from the gradual accumulation of amyloid β (Aβ) peptide, derived from amyloid precursor protein (APP) by the sequential actions of β and γ secretases (3). It is also interesting to note that Aβ has been implicated to play a vital role in the pathogenesis of traumatic brain injury (4), cerebral amyloid angiopathy (5), glaucoma (6), and Down syndrome (7). As for AD, there are no effective treatment strategies for these disorders. It has been discovered recently that the A673T coding mutation in APP protects significantly against memory decline in patients with AD and in the normal aging population by decreasing Aβ levels (8). These findings provided unequivocal evidence of the role of APP metabolism as a cause of not only familial but also sporadic cases of AD. However, the recent failure of secretase inhibitors in clinical trials because of toxicity indicates the urgent need for the identification of all proteins that regulate or modulate Aβ generation *in vivo*.

In recent years, substantial evidence has also accumulated to suggest that loss of synapses is the best pathological correlate of not only cognitive impairment in AD (9–11) but also in frontotemporal dementia (12, 13), dementia with Lewy bodies (14, 15), and normal aging (16, 17). However, which molecular pathways are responsible for synaptic loss is poorly understood. In a recent study, RanBP9 has been found to be within the clusters of RNA transcript pairs associated with markers of AD progression (18), suggesting that RanBP9 might contribute to the pathogenesis of AD. In fact, we demonstrated previously that RanBP9 is an important component of a multiprotein complex involving LRP, BACE1, and APP that robustly increased Aβ levels (19, 20) and substantially reduced synaptic proteins (21–25) because of reduced dendritic intersections and spine density (26), consequently leading to severe deficits in learning and memory performance in APΔE9 mice overexpressing RanBP9

* This work was supported, in whole or in part, by National Institute on Aging (NIA)/National Institutes of Health Grant R01AG036859-01 (to M. K. L.).
[1] To whom correspondence should be addressed: Torrey Pines Institute for Molecular Studies, 11350 S.W. Village Parkway, Port Saint Lucie, FL 34987-2352. Tel.: 772-345-4698; Fax: 772-345-3649; E-mail: mlakshmana@tpims.org.
[2] The abbreviations used are: AD, Alzheimer disease; Aβ, amyloid β; APP, amyloid precursor protein; LRP, low-density lipoprotein receptor-related protein; CHAPSO, 3-[(3-cholamidopropyl)dimethylammonio]-2-hydroxy-1-propanesulfonic acid; CTF, C-terminal fragment; sAPP, soluble amyloid precursor protein.

(23, 25). We also recently identified COP9 constitutive photomorphogenic homolog subunit 5 (COPS5, Jab1) as a *bona fide* binding partner of RanBP9 (27). To understand the role of COPS5 *in vivo* in the amyloidogenic processing of APP, we successfully generated and characterized transgenic mice overexpressing FLAG-COPS5. Here we show that COPS5 increases the amyloid plaque burden in the APΔE9 mouse model of AD and decreases the postsynaptic marker spinophilin *in vivo*. Therefore, we are establishing and defining the role of the members of a novel multiprotein complex that plays a vital role in both Aβ generation and synaptic deficits.

EXPERIMENTAL PROCEDURES

Chemicals and Antibodies—Thioflavin S (catalog no. T1892), paraformaldehyde (catalog no. P6148), glutaraldehyde (catalog no. G-7776), and protease inhibitor mixture for use in mammalian cells (catalog no. P8340) were purchased from Sigma-Aldrich. The polyclonal antibodies CT15 (against the C-terminal 15 residues of APP) and 63d (against the APP ectodomain) have been described previously (20). The monoclonal antibody 6E10 (catalog no. SIG-39300, recognizing 1–17 of the Aβ sequence) was obtained from Covance Research (Denver, CO). Polyclonal anti-sAPPβ-WT antibody (catalog no. 18957) was purchased from IBL Co. Ltd. (Gunma, Japan). Monoclonal antibody against RanBP9 was produced by immunizing mice with a peptide corresponding to amino acids 146–729 of RanBP9 as described previously (20). Anti-FLAG tag antibody (M2, catalog no. F3165) was purchased from Sigma. Anti-Jab1 rabbit monoclonal antibody (catalog no. 5156-1) was purchased from Abcam (Cambridge, MA). Mouse monoclonal anti-JAB1 antibody, clone 2A10 (catalog no. NB120-495) was purchased from Novus Biologicals (Littleton, CO). Anti-BACE1 monoclonal antibody (catalog no. H00023621-Mo2) was obtained from Abnova (Taipei, Taiwan). The polyclonal antibody 1704, recognizing the cytoplasmic domain of human LRP, has been described previously (20). Mouse monoclonal antibody against β-actin (catalog no. A00702) was purchased from Genscript USA Inc. (Piscataway, NJ). Anti-spinophilin (catalog no. 9061S) was from Cell Signaling Technology (Danvers, MA). All secondary antibodies were purchased from Jackson ImmunoResearch Laboratories (West Grove, PA). All antibodies for immunoblot analysis were diluted in 5% nonfat milk in Tris-buffered saline with 0.1% Tween 20 (TBS-T).

Generation of FLAG-COPS5 Transgenic Mice—The Addgene plasmid FLAG-HA-COPS5 (catalog no. 22541) was used as the source of human COPS5 cDNA. The COPS5 cDNA was PCR-amplified using the following primers: forward, 5′-cggaattcatggcggcgtccgggagcggt-3′; reverse, 5′-gcgtcgacttaagagatgttaatttgatt-3′. The 1005 bp of amplified DNA was cloned into the EcoRI and SalI restriction sites in fusion with the 3× FLAG sequence of p3×FLAG-CMV-7.1 plasmid (catalog no. E4026, Sigma-Aldrich). The 3×FLAG-COPS5 cDNA was released by restriction digestion and cloned in fusion with the mouse thy-1 promoter at the XhoI restriction site in the pTSC21K plasmid (provided by Prof. J. W. Gordon, New York, NY), which we have used previously for the successful generation of RanBP9 transgenic mice (21). The Thy-1 promoter restricts protein expression to the postnatal/adult brain so that any adverse effects of COPS5 during embryonic development can be avoided. The correct cloning was verified by sequencing, and protein expression was confirmed by immunoblots using both FLAG antibody and COPS5-specific antibody. The construct was linearized by digestion with NotI enzyme, which removed 2349 bp of vector backbone. The microinjection of cloned and linearized cDNA in to the blastocyst was carried out at the Sylvester Comprehensive Cancer Center Transgenic Core Facility (University of Miami) using standard techniques by strictly following animal use protocols as approved by the Animal Care and Use Committee at the Torrey Pines Institute for Molecular Studies in accordance with National Institutes of Health guidelines. The linearized thy-1.2-FLAG-COPS5 construct was microinjected into the pronuclei of fertilized C57BL/6 mouse eggs and reimplanted in the oviduct of pseudopregnant recipient mice. From over 75 pups born of eight mothers, genomic DNA was isolated from tails at the time of weaning, and positive mice were identified by genotyping for the transgene. The COPS5-specific primers used in the PCR were as follows: forward, 5′-gac tac aaa gac cat gac ggt-3′; reverse, 5′-cca ccc gat tgc att ttc aag-3′. The positive founder mice were then backcrossed with native C57bl/6 mice, and the colonies were expanded.

APΔE9/COPS5-Tg mice were generated by crossing heterozygous line 1903 of COPS5-Tg mice with the heterozygous B6.Cg-Tg, APPswe, PSEN1ΔE9 (APΔE9) double-transgenic mice (strain C57BL/6XC3H, F2) used as a robust model of AD obtained from JAX Laboratories (stock no. 005864).

Immunohistochemistry—Immunohistochemical stainings were performed in COPS5-Tg and WT mice with FLAG antibody and spinophilin antibody following protocols as described previously (23). Briefly, the primary antibody was incubated overnight, and the immunoreactivity was visualized using Alexa Fluor (488 or 568)-conjugated anti-rabbit or anti-mouse secondary antibodies. Coverslips were mounted on Vectashield mounting medium with DAPI (Vector Laboratories, Burlingame, CA), and images were obtained using a confocal microscope (C1Si laser-scanning multispectral confocal microscope, Nikon, Melville, NY). The images were converted in to grayscale, 8 pixels, and the density of spinophilin was quantified using Image-pro software.

Quantitation of Aβ in Mouse Brains by ELISA—To quantify the levels of Aβ40 and Aβ42 in the APΔE9 and APΔE9/COPS5-Tg genotypes, sandwich ELISA was used. Mice were euthanized by isoflurane, and cortical and hippocampal brain regions were separated, weighed, and homogenized in 1% CHAPSO/PBS with protease inhibitors. The homogenate was centrifuged at 100,000 × *g* for 1 h at 4 °C, and the supernatants were used for the quantitation of CHAPSO-soluble Aβ. The pellets were extracted with formic acid and used for measurement of Aβ by sandwich ELISA exactly as described previously by our laboratory (20, 21).

Staining of Amyloid Plaques—APΔE9 and APΔE9/COPS5-Tg genotypes of mice were anesthetized by isoflurane and perfused using a mixture of 4% paraformaldehyde and 0.02% glutaraldehyde in phosphate-buffered saline. The rest of the protocol was exactly as published previously (21, 25).

Quantitation of APP Holoprotein, C-terminal Fragments (CTFs), and sAPPs in Mouse Brains by Immunoblotting—Two genotypes of mice, viz. APΔE9 and APΔE9/COPS5-Tg mice, were euthanized with isoflurane and decapitated immediately, and cortical and hippocampal brain regions were rapidly separated into Tris buffer lacking any detergent (50 mM Tris-HCl (pH 7.4), 175 mM NaCl, and 5 mM EDTA) containing complete protease inhibitor mixture for use with mammalian cell and tissue extracts (Sigma). Tissue was homogenized using Power Gen 125 (Fisher Scientific, Pittsburgh, PA) and centrifuged at 100,000 × *g* for 1 h in a Beckman ultracentrifuge. The supernatant was used as the source of soluble proteins such as sAPPα and sAPPβ. The remaining pellet was dissolved in 1% Nonidet P-40 buffer (50 mM Tris-HCl (pH 8.0), 150 mM NaCl, 0.02% sodium azide, 400 nM microcystine-LR, 0.5 mM sodium vanadate, and 1% sodium Nonidet P-40) containing complete protease inhibitor mixture. After centrifugation, the supernatants were used to measure the levels of APP holoprotein, CTF-α, CTF-β, LRP-β chain, BACE1, COPS5, and RanBP9. The protocols for SDS-PAGE electrophoresis, chemiluminescent detection, and ImageJ quantitation of signals were exactly as described previously (20–26).

Behavioral Testing for Spatial Memory by T Maze—The spatial learning and memory skills in three genotypes of mice, *i.e.* WT, APΔE9, and APΔE9/COPS5-Tg, were assessed at 12 months of age by T maze paradigm exactly as described previously (23). Briefly, in this paradigm, mice are initially trained to learn a given task (acquisition) and, when the mice have learned the skill, are subjected to a probe test after a gap period to assess their ability to retain the learned task. We tested six mice per genotype in five sessions and ten trials per session. The probe test was conducted after a gap of 3 days.

Statistical Analysis—Immunoblot signals for APP holoprotein, CTFs, sAPPs, COPS5, RanBP9, and actin were quantified using ImageJ software. Statistical significance was established by Student's *t* test using Instat3 software (GraphPad Software, San Diego, CA). We used two-tailed *p* values, assuming that populations may have different standard errors. The data presented are mean ± S.E. The data were considered significant only when the *p* value was <0.05 (*, $p < 0.05$; **, $p < 0.01$; ***, $p < 0.001$).

RESULTS

Characterization of COPS5-Tg Mice—The design of the construct used to generate FLAG-COPS5 transgenic mice is shown schematically in Fig. 1*A*. Use of the Thy-1 promoter ensured expression of the transgene only in the postnatal period in the brain. The FLAG tag was used to differentiate endogenous COPS5 from exogenous FLAG-COPS5 expression. Following successful pronuclear injections, we identified and expanded three founder lines of mice. Both body and brain weights of FLAG-COPS5 mice did not differ from WT littermate controls (data not shown). Further analysis by routine histology by staining coronal and sagittal sections of the brain with H&E did not reveal any abnormality. The FLAG-COPS5 mice looked healthy, and no behavioral abnormalities of any kind were noted.

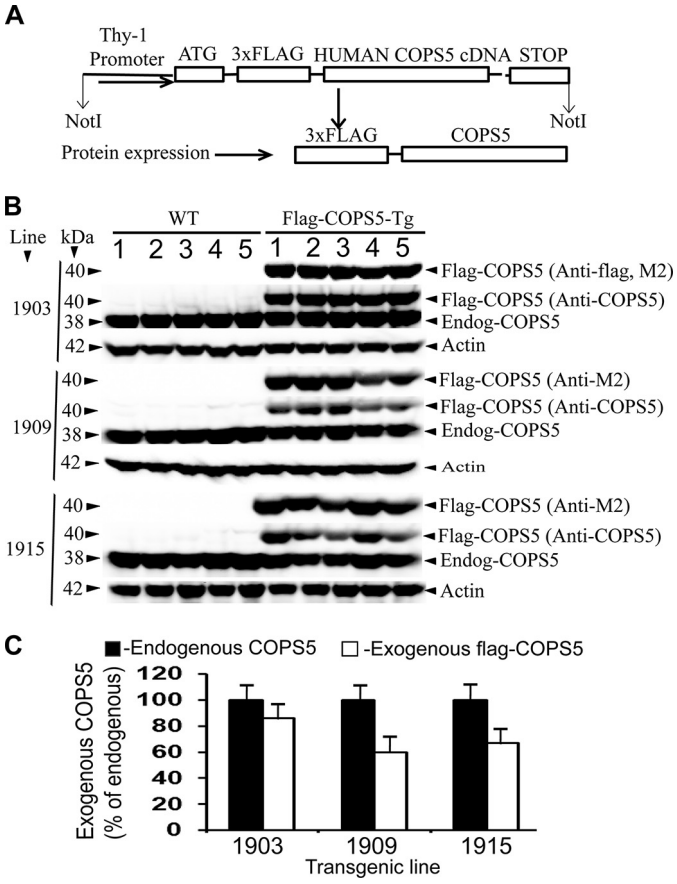

FIGURE 1. **Generation and immunoblot characterization of transgenic mice overexpressing FLAG-COPS5.** *A*, the construct used in the generation of transgenic mice. PCR-amplified human COPS5 cDNA was fused in frame with a 3× FLAG sequence and expressed under the control of the thy-1 promoter, which restricts protein expression only to the central nervous system and only during the postnatal period. *B*, immunoblots of 1% Nonidet P-40 lysates from WT mice or derived from three lines of transgenic mice at 12 months of age showing expression of FLAG-COPS5 in the cortex (*1*), hippocampus (*2*), thalamus (*3*), brainstem (*4*), and cerebellum (*5*). Exogenous FLAG-COPS5 was detected by FLAG antibody (M2), and both endogenous and exogenous COPS5 were detected by anti-COPS5 antibody. Actin was detected as a loading control. *C*, quantitation of COPS5 protein showed 86% in line 1903, 60% in line 1909, and 67% in line 1915 relative to the endogenous levels.

We characterized three lines of COPS5 transgenic mice derived from three founder lines, 1903, 1909, and 1915, by immunoblot analysis for the expression of the transgene using standard procedures. We used FLAG tag antibody (M2) to detect exogenous FLAG-COPS5 and COPS5-specific antibody to detect both exogenous and endogenous COPS5 (Fig. 1*B*). Line 1903 expressed about 1-fold FLAG-COPS5 protein relative to the endogenous COPS5 levels equally in all brain regions studied, *i.e.* cortex (*1*), hippocampus (*2*), thalamus (*3*), brainstem (*4*) and cerebellum (*5*) (Fig. 1*B*). FLAG antibody did not detect any signals in WT brains, suggesting that the signals seen in the FLAG-COPS5 mice are specific to FLAG-COPS5 fusion protein. Line 1909 expressed lower levels of the transgene in the brainstem and the cerebellum, whereas line 1915 expressed slightly lower levels in the thalamus (Fig. 1*B*). Quantitation and relative comparison of expression levels showed 86% in line 1903, 60% in line 1909, and 67% in line 1915 relative to the endogenous levels (Fig. 1*C*). Therefore,

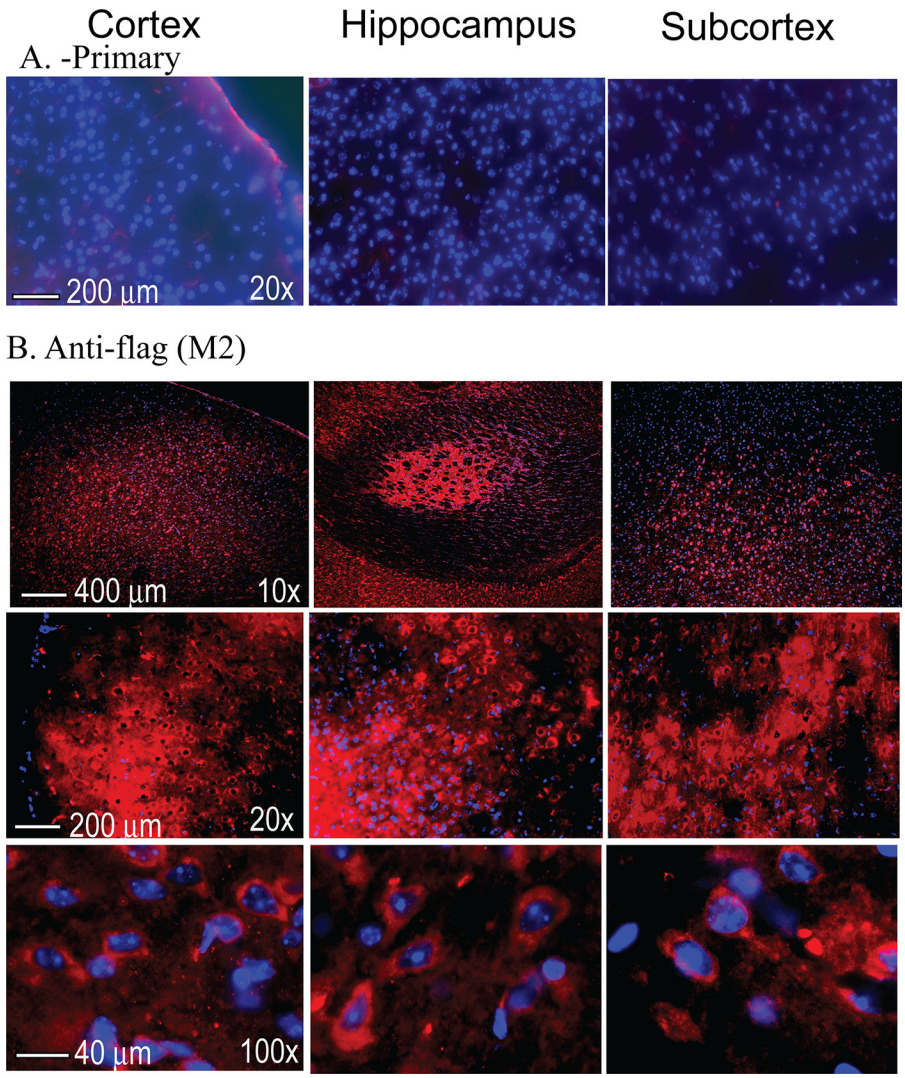

FIGURE 2. **Confocal images of the widespread expression of FLAG-COPS5 in transgenic line 1903 at 12 months of age.** *A*, negative controls without primary antibody showed no signals for FLAG-COPS5 (*red*) but showed only DAPI-stained nuclei (*blue*). *B*, different brain regions showing expression of FLAG-COPS5 stained immunohistochemically with FLAG antibody (M2). Images (×100) demonstrate the expression of FLAG-COPS5 mostly in the cytoplasm.

because line 1903 expressed the maximum level of exogenous FLAG-COPS5 of the three lines, we used line 1903 for all of our subsequent experiments, including immunohistochemical characterization.

To confirm the expression of FLAG-COPS5 by another method and to understand the pattern of expression distribution in the brain, we also stained line 1903 mouse brains by immunohistochemistry using FLAG antibody, which has the advantage of staining only the expression of FLAG-COPS5. We also used mounting medium with DAPI to stain the nuclei of neurons in the brain. Similar to the immunoblot results, we confirmed the widespread expression of FLAG-COPS5 in all brain regions examined. Fig. 2*B* shows staining at different magnifications in the cortex, hippocampus, and subcortical regions of the brain. Confocal images at a higher magnification (×100) clearly shows FLAG-COPS5 expression almost exclusively in the cytoplasm. Brain sections only stained with secondary antibody showed only DAPI-stained nuclei (blue) in the cortex, hippocampus, and subcortical areas of the brain (Fig. 2*A*), suggesting that the signals seen with FLAG antibody in Fig. 2*B* are specific to FLAG-COPS5 expression. Therefore, we successfully established transgenic mice with overexpression of FLAG-COPS5 in the brain.

COPS5 Overexpression Increases Aβ Levels and Amyloid Plaque Burden in the Mouse Brain—Because COPS5 overexpression in cell cultures led to a robust increase in Aβ levels (27), we were first interested to confirm whether such an effect is also seen *in vivo* in the mouse brain. Aβ was extracted from both CHAPSO-soluble and formic acid-soluble fractions from the brains of APΔE9/COPS5 and APΔE9 mice at both 6 and 12 months of age. Because the results were consistent in both fractions, quantitative data are only shown for CHAPSO-soluble Aβ. COPS5 overexpression in APΔE9 mice at 6 months of age increased Aβ40 levels by 32% ($p < 0.01$) and 28% ($p < 0.01$) in the cortex and hippocampus, respectively. The levels of Aβ42 were also increased in the same brain regions by 37% ($p < 0.05$) and 34% ($p < 0.05$), respectively (Fig. 3*A*). By 12 months of age, the increase was even more robust. Aβ40 levels were increased in the cortex by 63% ($p < 0.001$) and in the hippocampus by 65% ($p < 0.001$) compared with APΔE9 mice (Fig. 3*B*). Similarly,

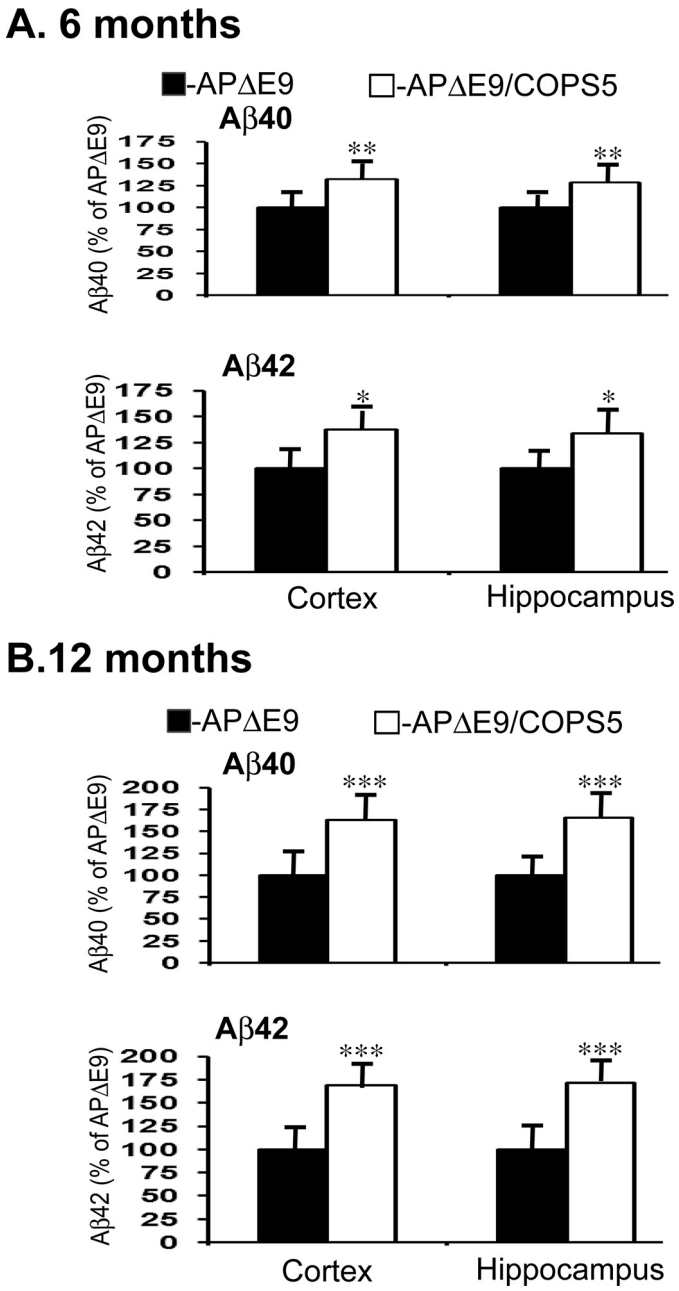

FIGURE 3. **COPS5 overexpression strongly increases Aβ levels *in vivo* at both 6 and 12 months of age.** *A*, CHAPSO-soluble Aβ40 and Aβ42 were extracted from cortical or hippocampal brain regions at 6 months of age and quantified by ELISA. Aβ40 levels were increased by 32% and 28% in the cortex and hippocampus, respectively, whereas the increase for Aβ42 levels in the same brain regions were 37% and 34% in APΔE9/COPS5 mice compared with APΔE9 mice. *B*, at 12 months of age, Aβ40 was increased in the cortex by 63% and in the hippocampus by 65% when COPS5 was overexpressed in APΔE9 mice. Similarly, Aβ42 was increased in the cortex by 69% and in the hippocampus by 71% when COPS5 was overexpressed in APΔE9 mice. Statistical analysis by Student's *t* test revealed significant differences. *, $p < 0.05$; **, $p < 0.01$; ***, $p < 0.001$. The data are mean ± S.E., and $n = 5$/genotype.

Aβ42 levels were also increased by COPS5 overexpression in APΔE9 mice by 69% ($p < 0.001$) in the cortex and by 71% ($p < 0.001$) in the hippocampus in relation to APΔE9 mice (Fig. 3*B*). Therefore, increased Aβ40 and Aβ42 levels by COPS5 were confirmed *in vivo* in the mouse brain.

To verify whether the increased Aβ levels by COPS5 lead to an increased amyloid plaque burden, amyloid plaques were

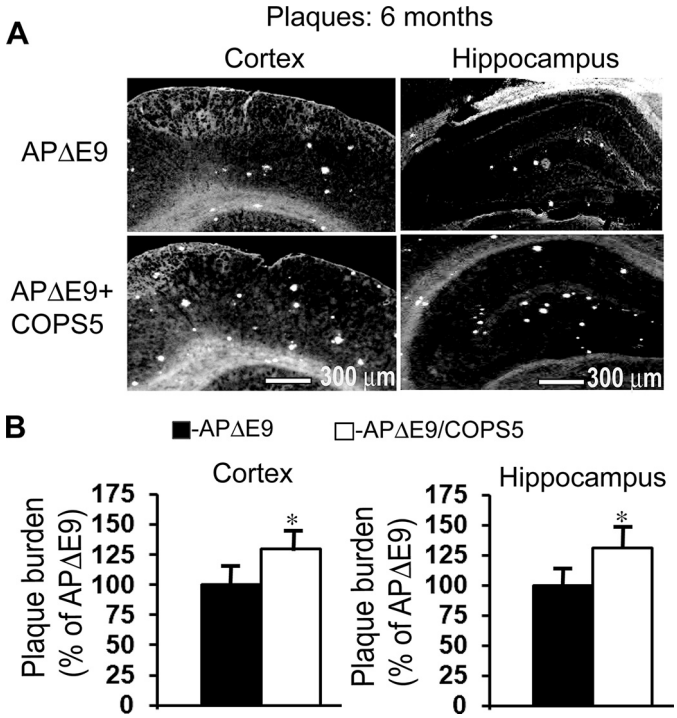

FIGURE 4. **COPS5 overexpression increases the amyloid plaque burden even by 6 months of age.** *A*, amyloid plaques were visualized by Thioflavin S staining and quantified by ImageJ. Representative images show an increased plaque burden in both the cortex and hippocampus because of COPS5 overexpression. *B*, plaques were quantified by ImageJ, which showed an increased burden in the cortex by 30% and in the hippocampus by 31% when COPS5 was overexpressed in APΔE9 mice. Statistical analysis by Student's *t* test revealed significant differences. *, $p < 0.05$. The data are mean ± S.E., and $n = 5$/genotype.

quantified in the same two genotypes of mice used for Aβ quantitation at both 6 and 12 months of age. Initially we quantified the number of plaques in the cortex and hippocampus of APΔE9 and APΔE9/COPS5-Tg genotypes, and then the plaque burden was calculated as the area occupied by plaques to the total region area. Even at 6 months of age, COPS5 overexpression in the APΔE9 mice significantly increased the amyloid plaque burden in both the cortex (30%, $p < 0.05$) and the hippocampus (31%, $p < 0.05$) (Fig. 4, *A* and *B*). At 12 months of age, compared with APΔE9 mice, COPS5 overexpression in APΔE9/COPS5-Tg mice increased the plaque burden by 54% ($p < 0.01$) in the cortex and by 64% ($p < 0.01$) in the hippocampus (Fig. 5, *A* and *B*). Therefore, both the cortex and the hippocampus appear to be equally vulnerable to the effects of COPS5 in increasing plaque burden.

COPS5 Overexpression Increases RanBP9, CTF-β, and sAPPβ and Decreases CTF-α and sAPPα Levels—COPS5 overexpression in NT2 cells robustly increased RanBP9 protein by inhibiting its degradation, thereby stabilizing the protein levels (27). Therefore, we quantified RanBP9 protein levels to see whether the same is true *in vivo*. When COPS5 was overexpressed in APΔE9 mice, the increase were 63% ($p < 0.001$) and 67% ($p < 0.01$) in the cortex and hippocampus, respectively (Fig. 6, *A* and *B*), suggesting that APP/PS1 overexpression in APΔE9 mice potentiates RanBP9 expression in the presence of COPS5.

To assess the effect of COPS5 on other metabolites of APP, we quantified the levels of sAPPs and CTFs in the cortex and the

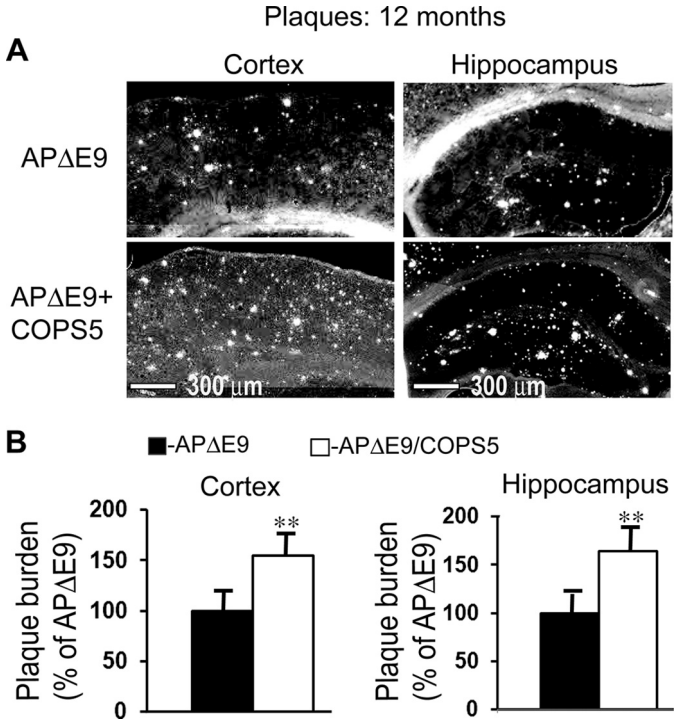

FIGURE 5. **COPS5 overexpression robustly increases the amyloid plaque burden at 12 months of age.** *A*, amyloid plaques were visualized by Thioflavin S staining and quantified by ImageJ. Representative images show an increased plaque burden in both the cortex and hippocampus because of COPS5 overexpression. *B*, the plaque burden, quantified by ImageJ, was increased in the cortex by 54% and in the hippocampus by 64% when COPS5 was overexpressed in APΔE9 mice. Statistical analysis by Student's *t* test revealed significant differences. **, $p < 0.01$. The data are mean ± S.E., and $n = 5$/genotype.

hippocampus. We used different antibodies to detect exogenous human APP and sAPPs and those of CTFs in APΔE9 mice. When comparing APΔE9 and APΔE9/COPS5-Tg mice, sAPPα levels (6E10) were decreased by 54% ($p < 0.01$) and 43% ($p < 0.01$), and sAPPβ levels (anti-sAPPβ, IBL) were increased by 67% ($p < 0.01$) and 106% ($p < 0.01$) in the cortex and hippocampus, respectively (Fig. 6, *A* and *B*). Consistent with changes in sAPPβ levels, CTF-β levels were also increased by about 37% in the cortex ($p < 0.05$) and the hippocampus ($p < 0.01$), whereas the levels of CTF-α were decreased significantly by 27% ($p < 0.05$) only in the cortex (Fig. 6, *A* and *B*). However, the levels of exogenous human APP holoprotein (CT15) were not altered when COPS5 was overexpressed in the APΔE9 mice. Therefore, COPS5 exerts an enormous influence on the amyloidogenic processing of human APP *in vivo* in the mouse brain.

COPS5 Overexpression Reduces Spinophilin-immunoreactive Puncta in the Adult Brain—To test whether increased amyloidogenic processing of APP by COPS5 leads to synaptic protein alterations in the adult brain, we quantified the spinophilin-immunoreactive puncta in a region of interest in the same genotypes of 12-month-old APΔE9/COPS5-Tg mice and compared them with those of APΔE9 mice. Consistent with the effect of RanBP9 on synaptic proteins, spinophilin numbers in the cortex were reduced by 19% ($p < 0.05$) in APΔE9/COPS5-Tg mice compared with APΔE9 mice (Fig. 7). The reduction in spinophilin levels in the hippocampus was about 20% ($p < 0.05$) in APΔE9/COPS5-Tg mice relative to APΔE9 mice (Fig. 7). These data indicate that COPS5 decreases postsynaptic protein *in vivo* in the adult brain, probably by up-regulating RanBP9.

COPS5 Overexpression in APΔE9 Mice Leads to Severe Deficits in Learning and Memory Skills at 12 Months of Age—To test whether reduced synapses by COPS5 in APΔE9 mice leads to learning deficits, we quantified and compared the percentage of correct responses and latency in the T maze paradigm in three genotypes of mice, *i.e.* WT, APΔE9, and APΔE9/COPS5-Tg. During acquisition on day 1, all three genotypes of mice showed a similar number of correct responses and latency. On day 2, although the number of correct responses remained similar in all the three genotypes of mice, latency was increased significantly in APΔE9 (15%, $p < 0.05$) and APΔE9/COPS5-Tg mice (17%, $p < 0.05$) compared with WT mice (Fig. 8*B*). On day 3, APΔE9/COPS5-Tg mice showed reduced correct responses compared with both WT (22%, $p < 0.01$) and APΔE9 mice (15%, $p < 0.05$). Latency was increased in both APΔE9 (18%, $p < 0.05$) and APΔE9/COPS5-Tg mice (25%, $p < 0.01$) compared with WT mice. On day 4, both APΔE9 (17%, $p < 0.05$) and APΔE9/COPS5-Tg mice (27%, $p < 0.01$) showed reduced correct responses compared with WT mice (Fig. 8*A*). The latency was also increased significantly by 13% ($p < 0.05$) and 24% ($p < 0.01$) in the APΔE9 and APΔE9/COPS5-Tg genotypes, respectively. On day 5 of acquisition, more robust differences were noticed for both correct responses and latency. APΔE9 mice showed a 20% ($p < 0.01$) decrease, whereas APΔE9/COPS5-Tg mice showed a 40% ($p < 0.001$) decrease in correct responses compared with WT mice. Importantly, there was a further 20% decrease in correct responses in APΔE9/COPS5-Tg mice when compared with APΔE9 mice. Similarly, latency was increased by 15% ($p < 0.05$) and 32% ($p < 0.001$) in APΔE9 and APΔE9/COPS5-Tg mice, respectively. Furthermore, there was 18% increased latency ($p < 0.01$) in APΔE9/COPS5-Tg mice compared with APΔE9 mice, suggesting that COPS5 overexpression further exacerbated learning deficits observed in APΔE9 mice.

Finally, the probe test also confirmed the negative influence of COPS5 on memory skills. Therefore, correct responses were reduced in APΔE9 mice (17%, $p < 0.05$) and APΔE9/COPS5-Tg mice (40%, $p < 0.001$) relative to WT mice (Fig. 8*A*). The increase in latency for these two genotypes of mice were 16% ($p < 0.05$) and 37% ($p < 0.001$), respectively (Fig. 8*B*). Interestingly, COPS5 overexpression in APΔE9 mice further worsened both correct responses (23%, $p < 0.01$) and latency (21%, $p < 0.01$) compared with APΔE9 mice. Therefore, COPS5 overexpression exacerbates learning and memory deficits in APΔE9 mice.

DISCUSSION

The primary objective of this study was to assess whether COPS5 plays any role in the amyloidogenic processing of APP, synaptic protein alterations *in vivo*, and learning and memory skills in mice. Our newly generated FLAG-COPS5 transgenic mice driven by the thy-1 promoter, which restricts COPS5 expression only to the central nervous system, were instrumental in successfully addressing these questions. Interestingly, we demonstrated that COPS5 increases β-site processing of APP

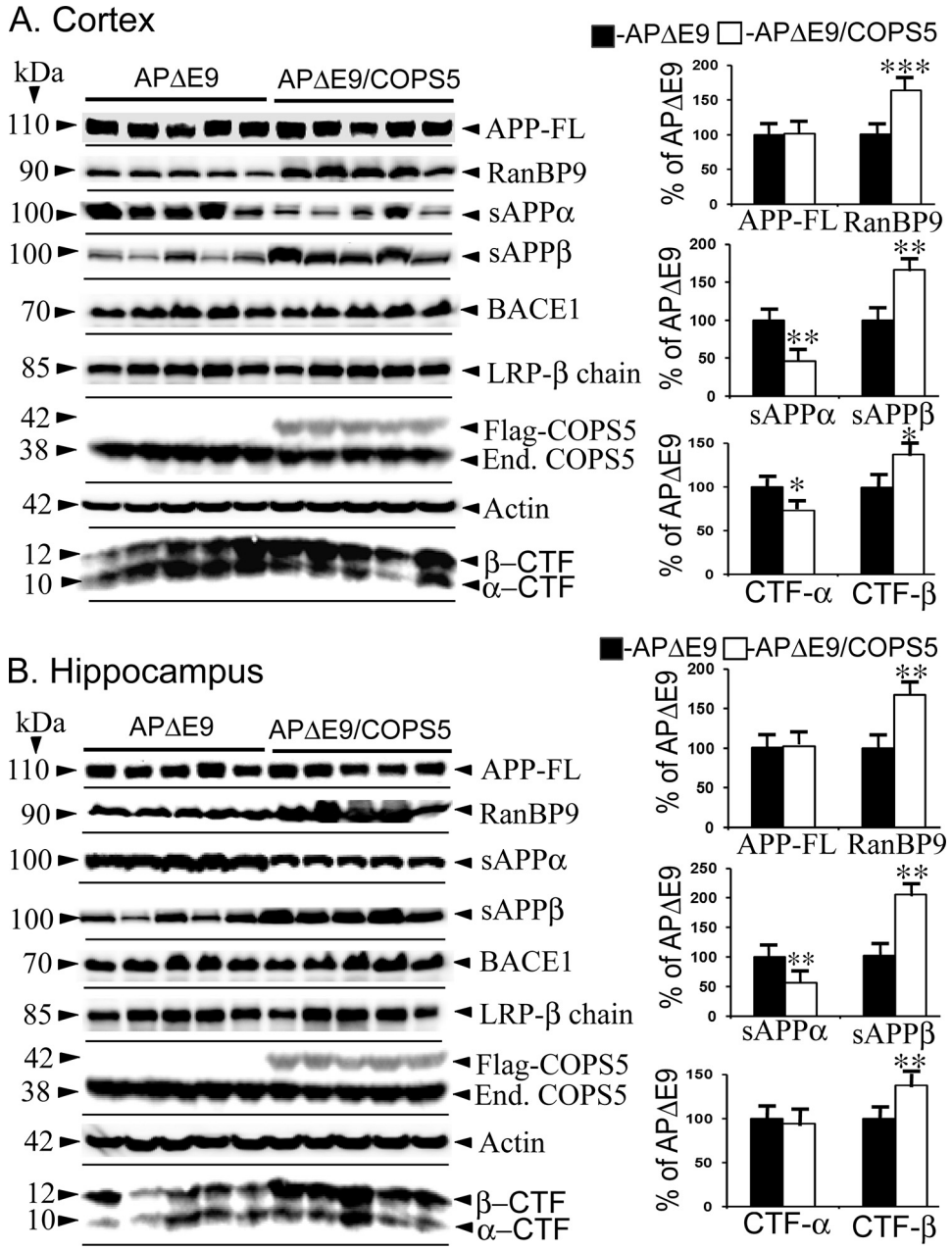

FIGURE 6. **COPS5 markedly alters endogenous levels of RanBP9 and exogenous levels of human sAPPα and sAPPβ without changing exogenous human APP holoprotein.** *A*, Nonidet P-40 lysates (for RanBP9, APP holoprotein, CTFs, BACE1, and LRP-β chain) or Tris lysates (for sAPPα and sAPPβ) were prepared from the cortex and subjected to immunoblotting. In the cortex of APΔE9/COPS5 mice, RanBP9 levels were increased by 63% and sAPPβ (anti-sAPPβ) levels by 67%, but the level of sAPPα (6E10) was reduced by 54% compared with APΔE9 mice. Similarly, CTF-β levels were increased by 37%, whereas CTF-α levels were decreased by 27% in APΔE9/COPS5 mice compared with APΔE9 mice. However, exogenous human APP holoprotein (CT15), BACE1, and LRP-β chain were unchanged. *End.COPS5*, endogenous COPS5. *B*, Nonidet P-40 or Tris lysates were prepared from the hippocampus and subjected to immunoblotting. Similar to the cortex, RanBP9 levels were increased by 67% and sAPPβ (anti-sAPPβ) levels by 106%, but the level of sAPPα (M3.2) was reduced by 43% in APΔE9/COPS5 mice compared with APΔE9 mice. Similarly, CTF-β levels were increased by 37%, whereas CTF-α levels were not altered significantly in APΔE9/COPS5 mice compared with APΔE9 mice. However, the levels of exogenous APP holoprotein (CT15), BACE1, and LRP-β chain were not altered. The data are expressed as percentage change from APΔE9 controls and were analyzed by Student's *t* test. **, $p < 0.01$; ***, $p < 0.001$. The data are mean ± S.E., and $n = 5$/genotype.

with the Swedish mutation *in vivo*, as reflected by increased sAPPβ generation in the APΔE9 mouse brains. Furthermore, COPS5 overexpression led to decreased levels of the marker of dendritic spines, *i.e.* spinophilin, in the adult brain. Most importantly, like RanBP9, COPS5 overexpression further exacerbated the learning and memory skill deficits observed in APΔE9 mice. Taken together, our data indicate that COPS5 is a novel member of the RanBP9 multiprotein complex that plays an essential role in Aβ generation and synaptic protein alterations *in vivo*.

We showed previously that COPS5 binds LRP, BACE1, APP, and RanBP9 in cell lines as well as in mouse brains, leading to a robust increase in the secretion of Aβ (27). The observation by others that both RanBP9 and COPS5 are present in the same subcellular fractions of the multiprotein complex (28) strengthened our conclusion that COPS5 is a novel member of the

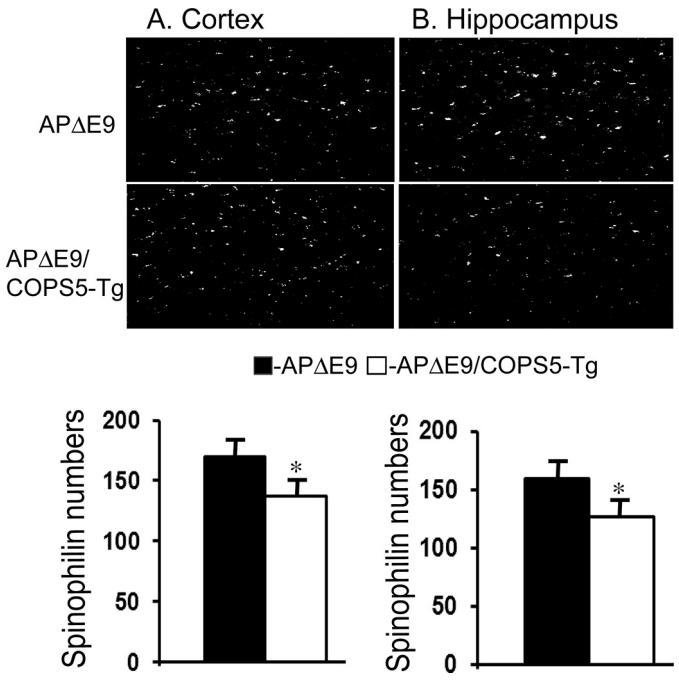

FIGURE 7. **Overexpression of COPS5 reduces spinophilin-immunoreactive puncta in the APΔE9 mouse brain in 12-month-old mice.** Coronal brain sections from APΔE9 and APΔE9/COPS5-Tg genotypes of mice were stained with spinophilin antibody and analyzed. Quantitation of the number of spinophilin puncta by Image-Pro in a region of interest in the brain showed reduced levels in APΔE9/COPS5-Tg mice by 19% in the cortex and by 20% in the hippocampus compared with APΔE9 mice. Statistical analysis by Student's *t* test revealed significant differences. *, $p < 0.05$. The data are mean ± S.E., and $n = 5$/genotype.

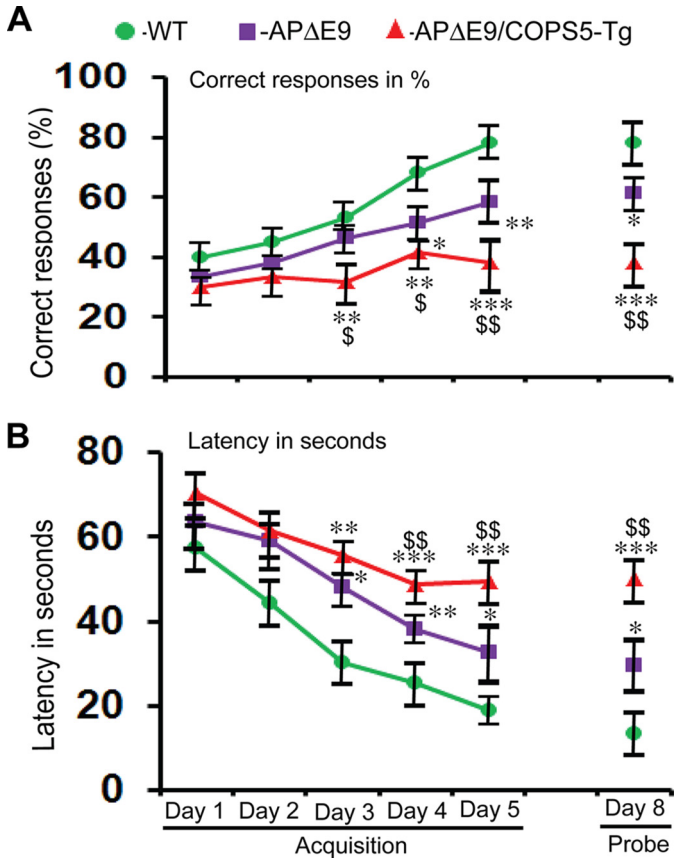

FIGURE 8. **Overexpression of COPS5 induces severe learning and memory deficits at 12 months of age in a T maze paradigm.** *A*, analysis of correct responses to reach the goal arm was plotted against the sessions, one session per day (10 trials per session) for 5 days, during acquisition and for the memory retention after a gap of 3 days during the probe test on day 8. B, analysis of latency in terms of time taken in seconds to reach the goal arm was plotted against the sessions as in *A*. APΔE9 mice showed significant deficits in both correct responses and latency during acquisition as well as memory retention. COPS5 overexpression in APΔE9 mice led to more severe deficits in both acquisition and memory retention. Repeated measures analysis of variance followed by post hoc Tukey-Kramer multiple comparison test revealed significant differences. *, $p < 0.05$; **, $p < 0.01$; ***, $p < 0.001$ compared with WT mice and $, $p < 0.05$; $$, $p < 0.01$ compared with APΔE9 mice. The data are mean ± S.E., and $n = 6$/genotype.

RanBP9 multiprotein complex involved in the processing of APP. Although COPS5 increased Aβ secretion almost 3-fold in cell cultures, an increase of only about 30% of both Aβ40 and Aβ42 even by 6 months of age, followed by a further increase of about 60% of both Aβ40 and Aβ42 at 12 months of age, *in vivo* in the APΔE9 mouse brains is even more significant. This is undoubtedly solid evidence to suggest that, like RanBP9, COPS5 also increases the amyloidogenic processing of APP *in vivo* in an age-dependent manner in the mouse brain. Perhaps an even more significant finding in this study is the up-regulation of RanBP9 protein levels in APΔE9/COPS5-Tg mice relative to APΔE9 mice. This implies that COPS5 increases Aβ generation and amyloid plaque burden by increasing RanBP9 protein levels through its stabilization. In N2A cells also, overexpression of COPS5 led to more than a 3-fold increase in RanBP9 protein levels (27). This is direct evidence that COPS5 acts through RanBP9 in increasing the amyloidogenic processing of APP. In this respect, it is worth noting that curcumin is a potent inhibitor of COPS5 (29), which might be responsible for a curcumin-mediated marked decrease in Aβ deposition in APP transgenic mice (30). Therefore, COPS5, like RanBP9, is an excellent molecular target to reduce Aβ generation.

Interestingly, the extent of increase in RanBP9 protein levels varied significantly with whether APP was coexpressed with COPS5. Therefore, increased RanBP9 protein levels in APΔE9/COPS5 mice were almost double the quantity seen in COPS5-Tg mice. This is consistent with our previous observation that RanBP9 protein levels are increased in both J20 (22) and APΔE9 (27) mouse brains compared with littermate controls. The exact reason for an increase in RanBP9 levels under APP overexpression conditions is not known, but such an increase was confirmed in the AD brains as well (23, 27, 31). Mechanistically, increased RanBP9, in turn, can enhance the functional interaction of LRP with APP or APP with BACE1, thereby enhancing lipid raft localization of APP, as we demonstrated previously (20). Because APP, BACE1, and γ-secretase components are all known to be present in the lipid rafts (32–34), increased lipid raft localization of APP by RanBP9/COPS5 can be expected to increase β site processing of APP. This is in line with a recent study that suggested that APP undergoes palmitoylation in its N-terminal E1 luminal domain and is preferentially targeted to lipid rafts, where it serves as a better BACE1 substrate initiating Aβ generation (35). The presence of enriched amounts of Aβ in lipid rafts in APP transgenic mice and human AD brains (36, 37) supports the enhanced amyloidogenic processing of APP in the lipid rafts. This, in turn, can account for increased Aβ generation by both RanBP9 and

COPS5, subsequently leading to an increased amyloid plaque burden. It remains to be determined whether COPS5, like RanBP9, is also present in lipid rafts. However, quantitations of CTF-β and CTF-α level were directly correlated to changes in sAPPβ and sAPPα levels in the cortex only. In the hippocampus, however, CTF-β levels were increased with no significant changes in CTF-α level upon COPS5 overexpression. These data also suggest that COPS5 may influence both β site processing of APP as well as indirectly through other mechanisms in the APΔE9 brains.

We also demonstrated that COPS5 overexpression reduces the dendritic spine marker spinophilin in adult mouse brains. The inverse correlation between increased RanBP9 levels and reduced spinophilin protein in both AD brains and APΔE9 mice observed previously in our laboratory (23) is consistent with this finding. Therefore, reduced synaptic proteins by COPS5 may simply be due to increased RanBP9. When RanBP9 protein levels are increased, it can increase bioenergetics defects at the nerve terminals (23), activate cofilin (22, 24, 25), and drastically reduce the growth and branching of dendritic processes in primary neurons (38) and adult brain (26), which can all account for reduced synaptic proteins by COPS5, leading to exacerbation of learning and memory skill deficits, as observed in this study. COPS5 is also known as CSN5 because it is the fifth component of the COP9 signalosome complex (39). In a previous study, the COP9 signalosome has been shown to inhibit the growth of dendritic branching through control of cullin3 function (40). Although the contribution of COPS5 was not delineated, it is very likely that COPS5 played a major role in the inhibition of dendritic branching because COPS5 is the main catalytic component of the COP9 signalosome. Furthermore, a significant quantity of COPS5 is also present in the cytosol, which markedly colocalizes with RanBP9 (27). We believe that it is this free form of COPS5 in the cytoplasm that is likely to form a complex with RanBP9 and play an important role in both Aβ pathology and synaptic protein alterations.

In AD, accumulation of amyloid plaques and loss of synapses are the major hallmarks of disease. Although the temporal sequence of these neuropathological events is under intense debate, we clearly demonstrated that COPS5 affects both mouse brain amyloid pathology and synaptic alterations by upregulating RanBP9 protein levels, which may be responsible for deficits in learning and memory skills. Importantly, COPS5 not only binds RanBP9, BACE1, LRP, and APP (27), which are all known to increase Aβ generation by targeting APP to lipid rafts, but we and others have shown previously that COPS5 binds LFA-1 (41, 42), and LFA-1, in turn, binds LRP (43). Interestingly, we also showed that RanBP9 increases endocytosis of LFA-1, LRP, and APP, thereby regulating cell adhesion and Aβ generation (44). By increasing endocytosis of LFA-1 and other integrins that are known to transduce synaptic plasticity signals, the COPS5/RanBP9 pathway may indirectly regulate synaptic alterations and behavioral deficits. RanBP9 also alters the phosphorylation of cofilin protein (22), one of the key regulators of actin dynamics and dendritic spine generation. This is also consistent with the integrin-LIMK pathway, which is also known to affect cofilin phosphorylation. Therefore, both COPS5 and RanBP9 bind several proteins playing an essential role in Aβ generation and synaptic plasticity. It is not clear, however, whether all of these proteins form a single multiprotein complex or several multiprotein complexes. The latter seems to be likely because both RanBP9 and COPS5 are present in several compartments of the cell, including the nucleus, the inner leaflet of the plasma membrane, and the cytoplasm, increasing the likelihood that they might interact with several local proteins to perform subcellular-specific functions. We recently demonstrated one such cell-specific protein complex involving RanBP9, LRP, and tyrosine receptor kinase AXl, where RanBP9 plays a central role in dendritic cell efferocytosis by scaffolding together these essential proteins (45). The structural organization of RanBP9 protein, consisting of several protein-protein interacting domains, makes it a perfect molecule to act as a scaffolding protein. COPS5 is also found in several protein complexes in which the binding is mediated by its conserved Mpr1p and PAD1p N-terminal domain. Another protein complex comprising COPS5, RanBP9, Ran, and Dyrk1b has been shown to regulate epithelial cell migration (28). Therefore, RanBP9 interaction with COPS5 appears to be vital for several cellular functions, most importantly in the amyloidogenic processing of APP and synaptic protein alterations, as described in this study. Therefore, we are establishing and unraveling the role of members of a novel multiprotein complex that plays a crucial role in the amyloidogenic processing of APP as well as synaptic damage and learning and memory skills. In the absence of a disease-modifying therapy for AD, it is significant that RanBP9 pathway molecules play a pivotal role in both Aβ generation and synaptic protein deficits. Small-molecule compounds that target the RanBP9 pathway, including COPS5, will be excellent novel therapeutic choices for AD. Reduced amyloid pathology by curcumin, which inhibits COPS5, is the best example of the proof of principle.

Acknowledgments—We thank the transgenic core facility at the Sylvester Comprehensive Cancer Center, University of Miami, for successful pronuclear injections. We also thank Dr. Wade Harper (Harvard Medical School) for the FLAG-HA-COPS5 construct (Addgene plasmid no. 22541).

REFERENCES

1. Wimo, A., Winblad, B., and Jönsson, L. (2010) The worldwide societal costs of dementia: estimates for 2009. *Alzheimers Dement.* **6,** 98–103
2. Selkoe, D. J. (2002) Alzheimer's disease is a synaptic failure. *Science* **298,** 789–791
3. Haass, C., Kaether, C., Thinakaran, G., and Sisodia, S. (2012) Trafficking and proteolytic processing of APP. *Cold Spring Harb. Perspect. Med.* **2,** a006270
4. Johnson, V. E., Stewart, W., and Smith, D. H. (2010) Traumatic brain injury and amyloid-β pathology: a link to Alzheimer's disease? *Nat. Rev. Neurosci.* **11,** 361–370
5. Smith, E. E., and Greenberg, S. M. (2009) β-Amyloid, blood vessels, and brain function. *Stroke* **40,** 2601–2606
6. Guo, L., Salt, T. E., Luong, V., Wood, N., Cheung, W., Maass, A., Ferrari, G., Russo-Marie, F., Sillito, A. M., Cheetham, M. E., Moss, S. E., Fitzke, F. W., and Cordeiro, M. F. (2007) Targeting amyloid-β in glaucoma treatment. *Proc. Natl. Acad. Sci. U.S.A.* **104,** 13444–13449
7. Nistor, M., Don, M., Parekh, M., Sarsoza, F., Goodus, M., Lopez, G. E., Kawas, C., Leverenz, J., Doran, E., Lott, I. T., Hill, M., and Head, E. (2007) α- and β-secretase activity as a function of age and β-amyloid in Down

syndrome and normal brain. *Neurobiol. Aging* **28,** 1493–1506
8. Jonsson, T., Atwal, J. K., Steinberg, S., Snaedal, J., Jonsson, P. V., Bjornsson, S., Stefansson, H., Sulem, P., Gudbjartsson, D., Maloney, J., Hoyte, K., Gustafson, A., Liu, Y., Lu, Y., Bhangale, T., Graham, R. R., Huttenlocher, J., Bjornsdottir, G., Andreassen, O. A., Jönsson, E. G., Palotie, A., Behrens, T. W., Magnusson, O. T., Kong, A., Thorsteinsdottir, U., Watts, R. J., and Stefansson, K. (2012) A mutation in APP protects against Alzheimer's disease and age-related cognitive decline. *Nature* **488,** 96–99
9. DeKosky, S. T., and Scheff, S. W. (1990) Synapse loss in frontal cortex biopsies in Alzheimer's disease: correlation with cognitive severity. *Ann. Neurol.* **27,** 457–464
10. Terry, R. D., Masliah, E., Salmon, D. P., Butters, N., DeTeresa, R., Hill, R., Hansen, L. A., and Katzman, R. (1991) Physical basis of cognitive alterations in Alzheimer's disease: synapse loss is the major correlate of cognitive impairment. *Ann. Neurol.* **30,** 572–580
11. Samuel, W., Masliah, E., Hill, L. R., Butters, N., and Terry, R. (1994) Hippocampal connectivity and Alzheimer's dementia: effects of synapse loss and tangle frequency in a two-component model. *Neurology* **44,** 2081-2088
12. Lipton, A. M., Cullum, C. M., Satumtira, S., Sontag, E., Hynan, L. S., White, C. L., 3rd, and Bigio, E. H. (2001) Contribution of asymmetric synapse loss to lateralizing clinical deficits in frontotemporal dementias. *Arch. Neurol.* **58,** 1233–1239
13. Sydow, A., Van der Jeugd, A., Zheng, F., Ahmed, T., Balschun, D., Petrova, O., Drexler, D., Zhou, L., Rune, G., Mandelkow, E., D'Hooge, R., Alzheimer, C., and Mandelkow, E. M. (2011) Reversibility of Tau-related cognitive defects in a regulatable FTD mouse model. *J. Mol. Neurosci.* **45,** 432–437
14. Masliah, E., Mallory, M., DeTeresa, R., Alford, M., and Hansen, L. (1993) Differing patterns of aberrant neuronal sprouting in Alzheimer's disease with and without Lewy bodies. *Brain Res.* **617,** 258–266
15. Brown, D. F., Risser, R. C., Bigio, E. H., Tripp, P., Stiegler, A., Welch, E., Eagan, K. P., Hladik, C. L., and White, C. L., 3rd (1998) Neocortical synapse density and Braak stage in the Lewy body variant of Alzheimer disease: a comparison with classic Alzheimer disease and normal aging. *J. Neuropathol. Exp. Neurol.* **57,** 955–960
16. Tigges, J., Herndon, J. G., and Rosene, D. L. (1996) Preservation into old age of synaptic number and size in the supragranular layer of the dentate gyrus in rhesus monkeys. *Acta. Anat.* **157,** 63–72
17. Uylings, H. B., and de Brabander, J. M. (2002) Neuronal changes in normal human aging and Alzheimer's disease. *Brain Cogn.* **49,** 268–276
18. Arefin, A. S., Mathieson, L., Johnstone, D., Berretta, R., and Moscato, P. (2012). Unveiling clusters of RNA transcript pairs associated with markers of Alzheimer's disease progression. *PLoS ONE* **7,** e45535
19. Lakshmana, M. K., Chen, E., Yoon, I. S., and Kang, D. E. (2008) C-terminal 37 residues of LRP promote the amyloidogenic processing of APP independent of Fe65. *J. Cell Mol. Med.* **12,** 2665–2674
20. Lakshmana, M. K., Yoon, I. S., Chen, E., Bianchi, E., Koo, E. H., and Kang, D. E. (2009) Novel role of RanBP9 in BACE1 processing of amyloid precursor protein and amyloid β peptide generation. *J. Biol. Chem.* **284,** 11863–11872
21. Lakshmana, M. K., Hayes, C. D., Bennett, S. P., Bianchi, E., Reddy, K. M., Koo, E. H., and Kang, D. E. (2012) Role of RanBP9 on amyloidogenic processing of APP and synaptic protein levels in the mouse brain. *FASEB J.* **26,** 2072–2083
22. Woo, J. A., Jung, A. R., Lakshmana, M. K., Bedrossian, A., Lim, Y., Bu, J. H., Park, S. A., Koo, E. H., Mook-Jung, I., and Kang, D. E. (2012a) Pivotal role of the RanBP9-cofilin pathway in Aβ-induced apoptosis and neurodegeneration. *Cell Death Differ.* **19,** 1413–1423
23. Palavicini, J. P., Wang, H., Bianchi, E., Xu, S., Rao, J. S., Kang, D. E., and Lakshmana, M. K. (2013) RanBP9 aggravates synaptic damage in the mouse brain and is inversely correlated to spinophilin levels in Alzheimer's brain synaptosomes. *Cell Death Dis.* **4,** e667
24. Wang, H., Wang, R., Xu, S., and Lakshmana, M. K. (2014a) RanBP9 overexpression accelerates loss of pre and postsynaptic proteins in the APΔE9 transgenic mouse brain. *PLoS ONE* **9,** e85484
25. Palavicini, J. P., Wang, H., Minond, D., Bianchi, E., Xu, S., and Lakshmana, M. K. (2014) RanBP9 overexpression down-regulates phospho-cofilin, causes early synaptic deficits and impaired learning, and accelerates accumulation of amyloid plaques in the mouse brain. *J. Alzheimers Dis.* **39,** 727–740
26. Wang, H., Lewsadder, M., Dorn, E., Xu, S., and Lakshmana, M. K. (2014) RanBP9 overexpression reduces dendritic arbor and spine density. *Neuroscience* **265,** 253–262
27. Wang, H., Dey, D., Carrera, I., Minond, D., Bianchi, E., Xu, S., and Lakshmana, M. K. (2013) COPS5 (Jab1)protein increases β site processing of amyloid precursor protein and amyloid β peptide generation by stabilizing RanBP9 protein levels. *J. Biol. Chem.* **288,** 26668–26677
28. Zou, Y., Lim, S., Lee, K., Deng, X., and Friedman, E. (2003) Serine/threonine kinase Mirk/Dyrk1B is an inhibitor of epithelial cell migration and is negatively regulated by the Met adaptor Ran-binding protein M. *J. Biol. Chem.* **278,** 49573–49581
29. Li, J., Wang, Y., Yang, C., Wang, P., Oelschlager, D. K., Zheng, Y., Tian, D. A., Grizzle, W. E., Buchsbaum, D. J., and Wan, M. (2009) Polyethylene glycosylated curcumin conjugate inhibits pancreatic cancer cell growth through inactivation of Jab1. *Mol. Pharmacol.* **76,** 81–90
30. Lim, G. P., Chu, T., Yang, F., Beech, W., Frautschy, S. A., and Cole, G. M. (2001) The curry spice curcumin reduces oxidative damage and amyloid pathology in an Alzheimer transgenic mouse. *J. Neurosci.* **21,** 8370–8377
31. Lakshmana, M. K., Chung, J. Y., Wickramarachchi, S., Tak, E., Bianchi, E., Koo, E. H., and Kang, D. E. (2010) A fragment of the scaffolding protein RanBP9 is increased in Alzheimer's disease brains and strongly potentiates amyloid-beta peptide generation. *FASEB J.* **24,** 119–127
32. Vetrivel, K. S., Cheng, H., Lin, W., Sakurai, T., Li, T., Nukina, N., Wong, P. C., Xu, H., and Thinakaran, G. (2004) Association of γ-secretase with lipid rafts in post-Golgi and endosome membranes. *J. Biol. Chem.* **279,** 44945–44954
33. Vetrivel, K. S., Cheng, H., Kim, S. H., Chen, Y., Barnes, N. Y., Parent, A. T., Sisodia, S. S., and Thinakaran, G. (2005) Spatial segregation of γ-secretase and substrates in distinct membrane domains. *J. Biol. Chem.* **280,** 25892–25900
34. Hattori, C., Asai, M., Onishi, H., Sasagawa, N., Hashimoto, Y., Saido, T. C., Maruyama, K., Mizutani, S., and Ishiura, S. (2006) BACE1 interacts with lipid raft proteins. *J. Neurosci. Res.* **84,** 912–917
35. Bhattacharyya, R., Barren, C., and Kovacs, D. M. (2013) Palmitoylation of amyloid precursor protein regulates amyloidogenic processing in lipid rafts. *J. Neurosci.* **33,** 11169–11183
36. Cheng, H., Vetrivel, K. S., Drisdel, R. C., Meckler, X., Gong, P., Leem, J. Y., Li, T., Carter, M., Chen, Y., Nguyen, P., Iwatsubo, T., Tomita, T., Wong, P. C., Green, W. N., Kounnas, M. Z., and Thinakaran G. (2009) *S*-palmitoylation of γ secretase subunits nicastrin and APH-1. *J. Biol. Chem.* **284,** 1373–1384
37. Vetrivel, K. S., Meckler, X., Chen, Y., Nguyen, P. D., Seidah, N. G., Vassar, R., Wong, P. C., Fukata, M., Kounnas, M. Z., and Thinakaran, G. (2009) Alzheimer disease Aβ production in the absence of *S*-palmitoylation-dependent targeting of BACE1 to lipid rafts. *J. Biol. Chem.* **284,** 3793–3803
38. Cheng, L., Lemmon, S., and Lemmon, V. (2005) RanBPM is an L1-interacting protein that regulates L1-mediated mitogen-activated protein kinase activation. *J. Neurochem.* **94,** 1102–1110
39. Seeger, M., Kraft, R., Ferrell, K., Bech-Otschir, D., Dumdey, R., Schade, R., Gordon, C., Naumann, M., and Dubiel, W. (1998) A novel protein complex involved in signal transduction possessing similarities to 26 S proteasome subunits. *FASEB J.* **12,** 469–478
40. Djagaeva, I., Doronkin, S. (2009) COP9 limits dendritic branching via Cullin3-dependent degradation of the Actin-crosslinking BTB-domain protein Kelch. *PLoS ONE* **4,** e7598
41. Bianchi, E., Denti, S., Granata, A., Bossi, G., Geginat, J., Villa, A., Rogge, L., and Pardi, R. (2000) Integrin LFA-1 interacts with the transcriptional coactivator JAB1 to modulate AP-1 activity. *Nature* **404,** 617–621
42. Perez, O. D., Mitchell, D., Jager, G. C., South, S., Murriel, C., McBride, J.,

Herzenberg, L. A., Kinoshita, S., and Nolan, G. P. (2003) Leukocyte functional antigen 1 lowers T cell activation thresholds and signaling through cytohesin-1 and jun-activating binding protein 1. *Nat. Immunol.* **4,** 1083–1092

43. Spijkers, P. P., da Costa Martins, P., Westein, E., Gahmberg, C. G., Zwaginga, J. J., and Lenting, P. J. (2005) LDL-receptor-related protein regulates β2-integrin-mediated leucocyte adhesion. *Blood* **105,** 170–177
44. Woo, J. A., Roh, S. E., Lakshmana, M. K., and Kang, D. E. (2012b) Pivotal role of RanBP9 in integrin-dependent focal adhesion signaling and assembly. *FASEB J.* **26,** 1672–1681
45. Subramanian, M., Hayes, C. D., Thome, J. J., Thorp, E., Matsushima, G. K., Herz, J., Farber, D. L., Liu, K., Lakshmana, M., and Tabas, I. (2014) An AXL/LRP-1/RANBP9 complex mediates DC efferocytosis and antigen cross-presentation *in vivo*. *J. Clin. Invest.* **124,** 1296–1308